Earth-Science Reviews 225 (2022) 103915

Contents lists available at ScienceDirect

Earth-Science Reviews

journal homepage: www.elsevier.com/locate/earscirev

Large-scale CO_2 removal by enhanced carbonate weathering from changes in land-use practices

Sibo Zeng [b], Zaihua Liu [a,c,*], Chris Groves [d]

[a] State Key Laboratory of Environmental Geochemistry, Institute of Geochemistry, Chinese Academy of Sciences, 550081 Guiyang, China
[b] Institute of Geological Sciences, Geophysics Section, Freie Universität Berlin, 12249 Berlin, Germany
[c] CAS Center for Excellence in Quaternary Science and Global Change, 710061 Xi'an, China
[d] Crawford Hydrology Laboratory, Western Kentucky University, 42101 Bowling Green, USA

ARTICLE INFO

Keywords:
CO2 removal
Carbonate weathering
Land-use changes
Global carbon cycle
Liming

ABSTRACT

Continental rock weathering exerts a negative feedback on global warming by removing atmospheric CO_2. Carbonate weathering contributes most of the dissolved inorganic carbon measured in inland waters, chiefly as HCO_3^-, though carbonate rock covers only a minor proportion of continental surface (~15%). The fast kinetics of carbonate weathering leads the trace carbonate to contribute greater HCO_3^- loads than silicate even in silicate catchments. Thus, the uses of carbonate powders on continental surface with silicate via agricultural liming can potentially enhance the CO_2 removal. Here, using an equilibrium modeling approach and results of the CMIP6 GCM model, we estimate the actual total CO_2 removal (*ATCR*) by the weathering of both carbonate bedrock and carbonate-rich soils, at the global scale. The potential CO_2 removal (*PCR*) which can be achieved by spreading carbonate powders on non-carbonate lands is also estimated. The results show that the *ATCR* at present is approximately 0.166 Gt yr^{-1}, which is similar to the previous result estimated from the global river data base. The *PCR* is 0.843 Gt yr^{-1}, five times the *ATCR*. Future climate and land-use changes may strongly increase the *ATCR*. Therefore, we suggest that carbonate weathering enhancement by land-use changes can potentially help mitigate the current climate trends.

1. Introduction

The rapid increase of atmospheric CO_2 concentration is considered as the major driving force of contemporary global warming and global water cycle intensification (Florides and Christodoulides, 2009; Huntington, 2006). Global climate and human land-use change have enhanced the rates of continental rock weathering in recent decades (Raymond et al., 2008; Gislason et al., 2009; Drake et al., 2018). Over geologic time scales the chemical weathering of continental rocks is a major means for the removal of atmospheric carbon dioxide (CO_2), a process that would be expected to lessen the magnitude of global warming (Berner et al., 1983; Liu et al., 2010). However, a full understanding of the mechanisms and the responses of continental weathering to the global change of the contemporary era is lacking. Such uncertainty impedes our understanding of the potential for atmospheric CO_2 removal by rock weathering, which limits our ability to consider exploitation of this geologic process to help mitigate global warming.

Chemical weathering liberates the alkaline components from silicate and carbonate rocks, mainly as HCO_3^- (the major species of dissolved inorganic carbon in freshwaters), via consumption of CO_2 that is primarily of atmospheric origin, thus sequestering the carbon in terrestrial waters and/or the oceans (Berner et al., 1983; Gaillardet et al., 1999). Chemical weathering of Ca-silicate rocks is thought to control the long-term global climate by drawing down atmospheric CO_2 concentration via precipitation of carbonate in the ocean sediments.

$$CO_2 + CaSiO_3 \rightarrow CaCO_3 + SiO_2 \quad (1)$$

This process could storage atmospheric CO_2 for millions of years (0.5 to 1 Myr time scale). Although silicates are the most abundant minerals widely distributed on continental surfaces, their relatively slow dissolution kinetics limits the rate of their removal of CO_2 (Liu et al., 2011). In comparison, carbonate weathering captures atmospheric CO_2 into waters mainly as the form of dissolved inorganic carbon (DIC) or HCO_3^-.

$$Ca_xMg_{1-x}CO_3 + CO_2 + H_2O \rightarrow xCa^{2+} + (1-x)Mg^{2+} + 2HCO_3^- \quad (2)$$

Carbonate weathering accounts for ~68% of the alkalinity measured

* Corresponding author at: State Key Laboratory of Environmental Geochemistry, Institute of Geochemistry, Chinese Academy of Sciences, 550081 Guiyang, China.
E-mail address: liuzaihua@vip.gyig.ac.cn (Z. Liu).

https://doi.org/10.1016/j.earscirev.2021.103915
Received 25 June 2021; Received in revised form 6 October 2021; Accepted 29 December 2021
Available online 5 January 2022

in the solute loads of the world's 60 largest rivers (Gaillardet et al., 1999) despite the comparatively small proportion (15.2%) of carbonate rock that outcrops on the continents (Goldscheider et al., 2020). However, this weathering process has not been considered as a significant mechanism for mitigating global warming, because the incorporated CO_2 may ultimately be released back into the atmosphere by carbonate precipitation in the oceans over geologically longtime scales (Berner and Berner, 2012). However, recent studies suggest that the role of carbonate weathering in global carbon cycle cannot be neglected on short timescales (<3 kyr, the turnover time of the oceans, Oki, 1999), because the fast kinetics of carbonate dissolution makes this process very sensitive to environmental perturbations (Dreybrodt, 1988; Gaillardet et al., 2019; Zeng et al., 2021). Approximately 10–20 times more fast weathering rate of carbonate mineral compared to silicate (Meybeck, 1986) results in a greater CO_2 removal potential in the short timescale which makes carbonate weathering have a more significant role than silicate weathering in controlling the global carbon cycle (Liu et al., 2011; Gaillardet et al., 2019). Moreover, a growing body of new evidence suggests that coupled carbonate weathering with aquatic photosynthesis (Liu et al., 2010, 2011, 2018, 2021) may also generate long-term carbon sequestration via sedimentation and burial of autochthonous organic carbon (AOC) formed by the aquatic biological uptake of HCO_3^- (DIC) in natural surface waters (the 'biological carbon pump effect', Einsele et al., 2001; Lerman and Mackenzie, 2005; Hain et al., 2014; Ma et al., 2014; Nõges et al., 2016) in the following reaction:.

$$CaCO_3 + CO_2 + H_2O \rightarrow Ca^{2+} + 2HCO_3^- \rightarrow CaCO_3 + x(CO_2 + H_2O) + (1-x)(CH_2O + O_2) \quad (3)$$

Thus, carbonate weathering may help to mitigate rates of global warming in both short and long-term timescales (Liu et al., 2011, 2018).

Studies in recent decades have recorded the significant role that even the trace quantities of carbonate minerals found in many silicate rocks can play in the aqueous geochemistry of silicate-dominated river basins (Blum et al., 1998; Jacobson et al., 2002; Hagedorn and Cartwright, 2010). The major contribution from carbonate weathering in such areas is due to the greater solubility and faster kinetics of carbonate weathering (generally at least one order of magnitude greater than silicate weathering) (Liu et al., 2011). Further evidence of this characteristic is the significant role of carbonate weathering in carbonate-rich soils found in silicate rock basins in the world's arid and semi-arid regions (Schlesinger, 1985). For example, the rich carbonate content in loess of the Yellow River region, China, has changed some silicate-dominated river basins to carbonate weathering control there (Wang et al., 2016). Given the widespread distribution of soil carbonates in silicate rock regions it is important to consider their total contribution to continental weathering loads.

For millennia, liming, or amending soil with powdered calcium carbonate, has been a common agricultural practice worldwide to counteract soil acidification and to ameliorate soil quality (Goulding, 2016). Liming improves the soil structure and hydraulic conductivity by leaching Ca^{2+} and increasing the ionic strength of soil solutions (Haynes and Naidu, 1998). The use of lime fertilizers on soils benefits plant productivity, soil biological productivity, soil carbon sequestration and soil respiration (Paradelo et al., 2015; Fornara et al., 2011). Agricultural land-uses have altered the continental weathering processes and weathering loads. Long-term land-use changes and management in the Mississippi River basin, for example, have increased the HCO_3^- flux there for 50 years, with liming practices in many cultivated watersheds contributing a large proportion of this rising flux (Raymond et al., 2008). Liming also generates the higher HCO_3^- exports found in many other U. S rivers (West and McBride, 2005; Oh and Raymond, 2006). Agricultural liming thus has been proposed as part of a broad strategy to sequestrate atmospheric CO_2 (Hamilton et al., 2007). Yet, there has been no work to estimate the contribution of large-scale liming (or the spreading of simple mechanically-ground carbonate powders) to continental weathering loads and its potential for CO_2 removal. Wide use of liming on non-carbonate rocks could extend the cover of the process to nearly 84.7% of the total continental land surface. Liming these areas could promote carbonate weathering and the HCO_3^- flux while enhancing crop productivity and increasing the soil organic carbon stock. A fundamental requirement for implementation of this strategy is to determine the soil carbonate threshold that transfers the river basin weathering regime from silicate-dominant to carbonate-dominant control. This value is crucial to such a large-scale strategy, while also helping to lower the costs of widespread, indiscriminate liming. Here we compare the river weathering loads of a global selection of river basins having large proportions of carbonate-rich soils. We focus on river basins with only minor amounts of carbonate rock itself, in order to exclude the bedrock carbonate impact and thus detect the soil carbonate threshold.

To quantify the carbonate-rich soil areas of the selected river basins, the latest FAO (Food and Agriculture Organization) world soil property map (Sanchez et al., 2009) and a new global carbonate rock aquifer map (Goldscheider et al., 2020) are used. We also adopt a new global modeling approach and use the outcomes of the latest Coupled Model Intercomparison Project (Phase 6) Global Climate Model (CMIP6 GCM) to estimate the actual total CO_2 removal by carbonate weathering (ATCR) in both global carbonate rock outcrops and carbonate-rich soils. The potential carbon removal (PCR) which could be achieved by increasing liming (or spreading carbonate powders) on the non-carbonate lands is also estimated. In addition, due to the high sensitivity of the global carbonate weathering carbon removal flux to changes of climate and land-use (Zeng et al., 2019), we analyze the responses of carbonate weathering to future global change on both carbonate and non-carbonate terrains. Based on our modeling, some potentially beneficial human land-use changes to efficiently accelerate CO_2 removal in different regions are identified and discussed.

2. Materials and methods

2.1. Carbonate weathering carbon removal estimation

Our estimation was based on the common equation of carbonate weathering loads (Liu et al., 2018), a carbonate weathering equilibrium model (Dreybrodt, 1988), and an ecologic process-based pCO_2 model (Zeng et al., 2019). This approach accounts for both climatic and anthropogenic factors by using the latest CMIP6 (Coupled Model Intercomparison Project Phase 6) GCM (Global Climate Model) outputs (Law et al., 2017; Ziehn et al., 2017). The carbonate weathering CO_2 removal was calculated from both global carbonate rock outcrops (Goldscheider et al., 2020) and carbonate-rich soils in non-carbonate rock regions (Sanchez et al., 2009). The universal equation for calculating carbonate weathering carbon removal flux can be expressed as follows (Liu et al., 2010; Liu et al., 2018):

$$CCRF = 0.5 \times 12 \times R \times [HCO_3^-] \quad (4)$$

Eq. (4) is the total load of CO_2-originated HCO_3^- from runoff (R, in m yr^{-1}), where $CCRF$ is the carbonate weathering carbon (CO_2) removal flux (in t C km^{-2} yr^{-1}), 0.5 indicates that only one half of the HCO_3^- generated by this process is of atmospheric origin, $[HCO_3^-]$ is the concentration of HCO_3^- (in mmol L^{-1}), 12 = the molar mass of carbon in g mol^{-1}.

2.2. Potential maximum carbonate dissolution equation

The calcium equilibrium concentration $[Ca^{2+}]_{eq}$ for a solution saturated with respect to calcite can be derived to very high accuracy from the analytical expression (Dreybrodt, 1988):

$$\left[Ca^{2+}\right]_{eq}^{3} = \frac{K_1 K_C K_H}{4 K_2 \gamma_{Ca^{2+}} \gamma^2_{HCO_3^-}} pCO_2 \quad (5)$$

where the temperature-dependent equilibrium constants for the relevant chemical reactions are K_1 and K_2 (the first and second dissociation constants for carbonic acid in water), K_c (the equilibrium constant for calcite dissolution), and K_H (Henry's Law constant for CO_2 gas in water), γCa^{2+} and γHCO_3^- are the activity coefficients for calcium and bicarbonate, respectively, and pCO_2 (in atm) is the CO_2 partial pressure. $[HCO_3^-]_{eq}$ is equal to 2 times $[Ca^{2+}]_{eq}$. Here, we assume that carbonate weathering is driven chiefly by calcite dissolution. Eq.(5) is valid for open-system conditions, where the solution is in the contact with atmosphere or CO_2-containing soils, and the CO_2 captured for dissolution is replenished from these two sources. Under closed system conditions for deep flow, however, CO_2 is not replenished, and the pCO_2 concentration in the solution decreases as dissolution proceeds. Hence, Eq.(5) cannot be directly applied. If p^iCO_2 is the partial pressure of CO_2 prior to any dissolution of calcite, then the pCO_2 at the closed system equilibrium is given by (Dreybrodt, 1988):

$$pCO_2 = p^iCO_2 - \frac{C_{eq}}{K_H\left(1 + \frac{1}{K_0}\right)} \quad (6)$$

which is valid for $p^iCO_2 > 7 \times 10^{-4}$ atm. K_0 the equilibrium constant for reaction of water and CO_2 to form carbonic acid.

2.3. Parameterized soil pCO_2

The soil pCO_2 model used in this study was introduced by Gwiazda and Broecker (1994) and Goddéris et al. (2010) and has been simplified in Gaillardet et al. (2019). This is a process-based model assuming that CO_2 is produced by soil biota respiration across the root zone. A power function is used to define the pCO_2 profile by solving the complete CO_2 diffusion equation in the soil layers. The soil pCO_2 below the deep roots equals approximately 75% of the ecosystem net primary production (*NPP*), i.e. the soil CO_2 reaches its maximum and becomes constant below an average rooting depth. Soil pCO_2 can thus be expressed as a function of atmospheric CO_2 concentration, temperature and *NPP*, as shown below:

$$pCO_{2(soil)} = pCO_{2(atm)} + \frac{A \times 0.75 \times NPP}{T^2} \quad (7)$$

where $A = 1.03 \times 10^6$, a conversion unit constant, $pCO_{2(atm)}$ is the atmospheric CO_2 pressure in ppmv, *NPP* is net primary production in grams of dry matter per meter square per year (g m^{-2} yr^{-1}), *T* is the surface temperature expressed in K and $pCO_{2(soil)}$ is the maximum CO_2 pressure reached below the root zone in ppmv.

2.4. Databases

To estimate the global *CCRF*, we applied the historical (2000–2014) and three GMIP6 future (2015–2100) model projections (SSP126-Sustainable paths, SSP245-Middle paths, SSP585-Development paths based on fossil fuels) for near-surface air temperature (*T*), runoff (*R*), net primary production (*NPP*) and cropland fraction from the Australia Community Climate and Earth System Simulator (ACCESS) (Law et al., 2017; Ziehn et al., 2017). The historical database was used to estimate the actual total carbon removal (*ATCR*) and its spatial distribution. The three future data projections were applied to analyze the trends and sensitivity of *CCRF* response to future global changes. In order to extract the carbonate weathering intensity in global carbonate rock areas, we used a new world karst aquifer map (WOKAM) which was provided by the Bundesanstalt für Geowissenschaften und Rohstoffe (BGR), International Association of Hydrogeologists (IAH), Karlsruhe Institute of Technology (KIT) and the United Nations Educational, Scientific, and Cultural Organization (UNESCO). This map provided the spatial distribution of global carbonate rocks, but it did not include carbonate rocks covered by later consolidated strata (Goldscheider et al., 2020). Due to the difficulties of precisely distinguishing limestone from the globally less common dolostone in the geological map, we calculated the carbonate weathering intensity by assuming that all carbonates are calcium carbonate (calcite). The Digital Soil Map of the World (DSMW) v3.6 amended by Food and Agricultural Organization of the United Nations (FAO) in 2007 was used to extract the distribution of global soil with rich carbonate content (Sanchez et al., 2009). These data were first used to determine the carbonate ($CaCO_3$) concentration threshold that would attribute a river's solute weathering loads to carbonate control, then to calculate the contributions of carbonate-rich soil carbonate weathering to *ATCR* in the carbonate-rich soils in non-carbonate rock areas.

2.5. Estimation of the global total area characterized by carbonate weathering control

Many water-stressed river basins in silicate rock areas develop accumulations of soil carbonate over geological time (Schlesinger, 1985). Great impacts of soil carbonate on total weathering loads have been found in these rivers. A prominent example is the Yellow River basin in China, where drought and high $CaCO_3$ content in loess have changed the river weathering loads from silicate-dominant to carbonate control. Although the river basin is dominated by silicate rocks, 90% of bicarbonate in the Yellow River is generated by carbonate weathering (Wang et al., 2016). Moreover, it was found that in the Narmada River and Tapti River (India), nearly 75% and 46% of HCO_3^-, respectively, derive from carbonate weathering, although there is no evidence of carbonate rock outcrops in these two river basins. The alkaline soil could be a major source for these high HCO_3^- loads (Sharma and Subramanian, 2008). In addition, there are no major carbonate rock outcrops in the Murray River basin of Australia (only 2.38%), while data there suggest a high proportion (34%) of carbonate weathering-driven dissolved load. Therefore, this is evidence that the carbonate contribution to the total weathering load of a given river can be influenced or even dominated by its areas of carbonate-rich soil, even in those basins with no mapped carbonate rock outcrops at all.

Previous studies have suggested that pedogenic calcite is widely present in global desert or semi-desert regions (mostly less than 1200 mm yr^{-1}, Fig. 1) (Adams, 1993). The thickness of soils with carbonate nodules is found to be correlated with mean annual range of precipitation (Retallack, 2005). An arid environment and highly irregular water supply favor accumulation of such secondary carbonate deposits. According to the latest digital FAO world soil map (Schlesinger, 1985), soils with rich carbonate content are mostly located in water-stressed areas. Therefore, we analyzed the relationships between global soil polygon carbonate content and annual mean precipitation. The carbonate content of soil polygons where precipitation is below 1200 mm yr^{-1} are mostly higher than >5%, while the pedogenic calcite contents are extremely low (generally <5%) in more humid regions (Fig. 1). We selected river basins with annual average precipitation lower than 1200 mm and carbonate rock outcrop less than 15% to test the relationship between carbonate weathering loads and areas of carbonate-rich soils. From the studies in these water-stressed river basins it was found that the fractions of carbonate weathering loads were positively related with their carbonate-rich soil areas where carbonate content is higher than 5% (Fig. 2 and Table 1). In addition, some river basins contain no mapped carbonate rocks or carbonate-rich soils at all but still have a small fraction of carbonate weathering products, which may be attributed to trace carbonate minerals in silicate rocks (Liu et al., 2011). Therefore, we presumed that 5% soil carbonate content was an acceptable baseline or threshold to identify a region that is dominated by carbonate weathering. As a consequence, we reclassified the soil polygons where carbonate content exceeds 5% (from the FAO digital world soil map) to define carbonate weathering control areas. The global areas

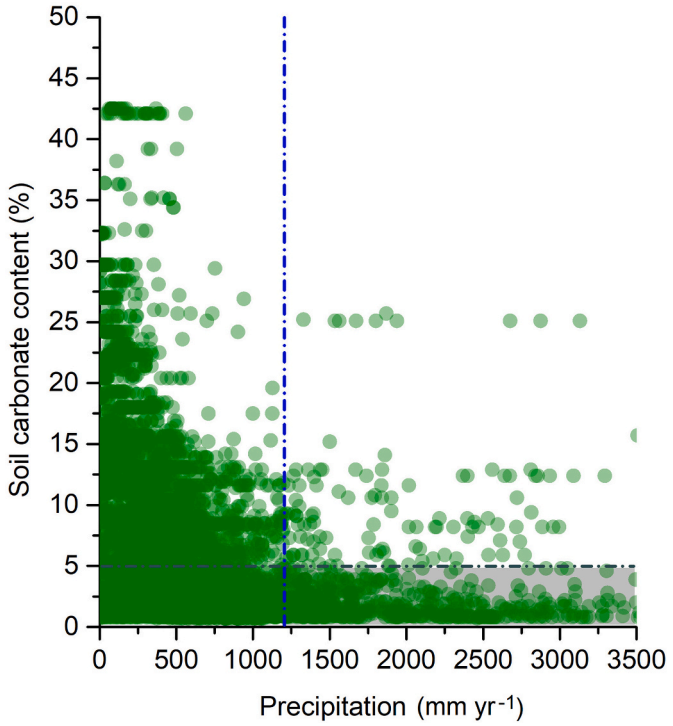

Fig. 1. Global soil carbonate contents plotted against mean annual precipitation. The soil polygons were extracted from the Digital Soil Map of the World (DSMW) v3.6 amended by the Food and Agricultural Organization of the United Nations (FAO) in 2007. Precipitation was the annual average of ACCESS historical output. The intercept of the dashed lines indicates the broad precipitation threshold of ~1200 mm yr^{-1} below which a rich soil carbonate content (>5%) can be readily formed.

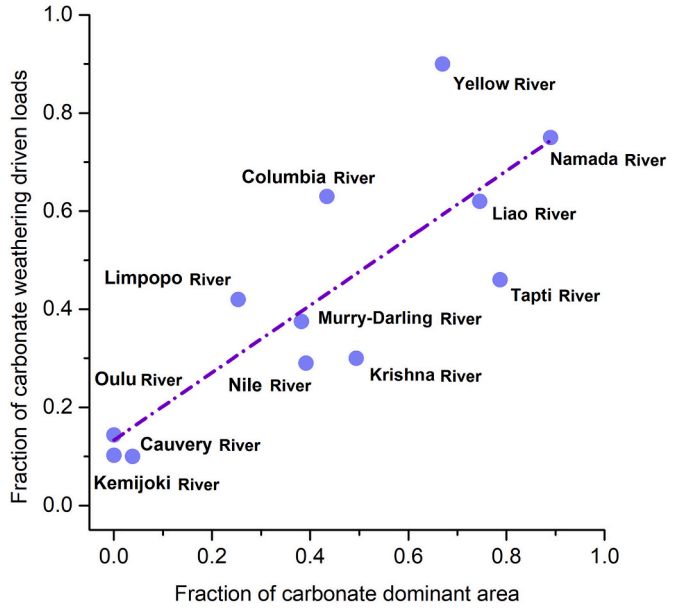

Fig. 2. The relationship between selected river basin carbonate weathering-driven loads and their carbonate-rich soil (>5%) areas. The selected rivers contained only minor carbonate rock outcrops (<15%, with an average of 4.8%) to highlight the influences of pedogenic carbonate weathering (Table 1).

characterized by carbonate-rich soils (with carbonate rock outcrops excluded) are expanded to 2.46 × 10^7 km^2, amounting to 16.7% of the continental surfaces. These carbonate-rich soils are mostly found in arid or semi-arid regions, especially in North Africa, the Middle East, North China and the western United States (Fig. 3). The global total area characterized by carbonate weathering control (carbonate rock + carbonate-rich soils in non-carbonate rock areas) was thus extended to 33.8% of the aggregate land surface, while other rocks or glaciers cover the remainder.

3. Results

3.1. The ATCR and PCR by carbonate weathering

Based on the new global carbonate area classification, the historical outcomes (2000–2014) of the Australian Community Climate and Earth System Simulator General Circulation Model (ACCESS GCM) and a new carbonate-weathering carbon removal flux (*CCRF)* approach, we first estimated the *CCRF* at the global scale, including all carbonate rock outcrops, carbonate-rich soils and non-carbonate areas (Fig. 4). High *CCRFs* were found in South America, Central Africa, Southwest China and Southeast Asia, whereas lowest *CCRFs* occurred in arid regions (North Africa, Middle East, Central Australia). The global annual mean *ATCR* in the carbonate areas (rock + soil) was approximately 0.166 Gt C yr^{-1}, which is similar to the previous result (0.148 Gt C yr^{-1}) estimated from the global river data base by Gaillardet et al. (1999). China, the U.S.A and Russia have the highest *ATCR* over the historical period due to their large national territories and areas of carbonate rock (Table 2). To quantify potential CO_2 removal by the spreading of carbonate powder on the non-carbonate land areas, we assumed that the remaining dry, ice-free land surface (66.17%) is fertilized with them. The calculated *PCR* is 0.843 Gt per year, about five times *ATCR*. The world's top three countries in *PCR* are Brazil, Russia and Colombia (Table 2).

(Fig. 4 and Table 2 here)

3.2. Global trends of ATCR and PCR by carbonate weathering

We next estimated the future trends of *ATCR* and *PCR* at the global scale by using the ACCESS outcomes of three representative CMIP6 scenarios - ssp126, ssp245 and ssp585 (Fig. 5). The future simulations showed significant *ATCR* enhancements in the global carbonate areas. From 2015 to 2100 CE, *ATCR* will likely increase by an average of 10% due to global changes (Fig. 5A). The *ATCR* trend is similar to our earlier global analysis which used the parameters from the CMIP5 GCM to estimate total carbon removal in the carbonate rock outcrop areas only (Zeng et al., 2019). In contrast, *PCR* is predicted to decline less than 1% up to 2100 (Fig. 5B). In the top ten nations with the highest *ATCR*, the greatest enhancement of carbon removal will likely occur in China, Russia and the U.S.A. (Fig. 5C). These three countries also showed significant increases of the *PCR* in their non-carbonate lands (Fig. 5D). In contrast, trends to decreasing *PCR* were found in Brazil, Columbia, Peru and Bolivia. These results indicated that the future carbonate weathering carbon removal flux will respond sensitively to global change (climate + land use), yet the impacts of this change may vary widely at the global scale.

4. Discussion

4.1. The climatic and anthropogenic drivers of spatial-temporal CCRF variations

The numerous climatic and anthropogenic drivers involved in continental weathering and their influences are highly intertwined in the field (Zeng et al., 2019; Beaulieu et al., 2012; Gaillardet et al., 2019). Climatic drivers are the key ones for those ecosystems where there are only minor anthropogenic impacts. Climate controls carbonate weathering rates via biotic and abiotic processes such as thermodynamic conditions, plant productivity, soil respiration and water supply. Temperature enters the carbonate equilibrium model and the *CCRF* model in

Table 1
Selected river basin carbonate weathering-driven loads and their carbonate-rich soil (>5%) areas. The selected rivers contained only minor carbonate rock outcrops (<15%, with an average of 4.8%) to highlight the influences of pedogenic carbonate weathering.

River basin	BA	CRA	CSA	P	CRF	CSF	TCF	ACWF
	(km^2)	(km^2)	(km^2)	mm yr^{-1}	(%)	(%)	(%)	(%)
Liao River[(1)]	274,646	12,264	192,491	630	4.47	70.09	74.55	75
Yellow River[(2)]	881,193	123,358	466,825	428	14.00	52.98	66.98	90
Krishna[(3)]	251,616	22,641	101,653	700	9.00	40.40	49.40	30
Murray-Darling[(4)]	1,049,016	24,931	375,960	400	2.38	35.84	38.22	38
Tapti[(5)]	73,780	0	52,287	1152	0.00	70.87	70.87	46
Cauvery[(6)]	91,056	1277	2259	1279	1.40	2.48	3.88	10
Namada[(5)]	95,805	8186	77,132	1138	8.54	80.51	89.05	75
Kemijoki[(7)]	52,270	0	0	491	0.00	0.00	0.00	14
Oulu[(7)]	34,178	0	0	556	0.00	0.00	0.00	10
Nile[(4)]	3,057,386	205,809	991,513	670	6.73	32.43	39.16	29
Limpopo[(4)]	413,588	22,581	82,156	490	5.46	19.86	25.32	42
Columbia[(4)]	670,165	78,297	212,763	636	11.68	31.75	43.43	63

Data: (1) Hu et al., 2017; (2) Wang et al., 2016; (3) Das et al., 2005; (4) Gaillardet et al., 1999; (5) Sharma and Subramanian, 2008; (6) Pattanaik et al., 2013; (7) Sun et al., 2017.
BA: Basin Area; CRA: Carbonate rock area; CSA: Carbonate-rich soil area; P: Precipitation; CRF: Carbonate rock fraction; CSF: Carbonate-rich soil fraction; TCF: Total carbonate-area fraction; ACWF: Actual carbonate-driven weathering fraction.

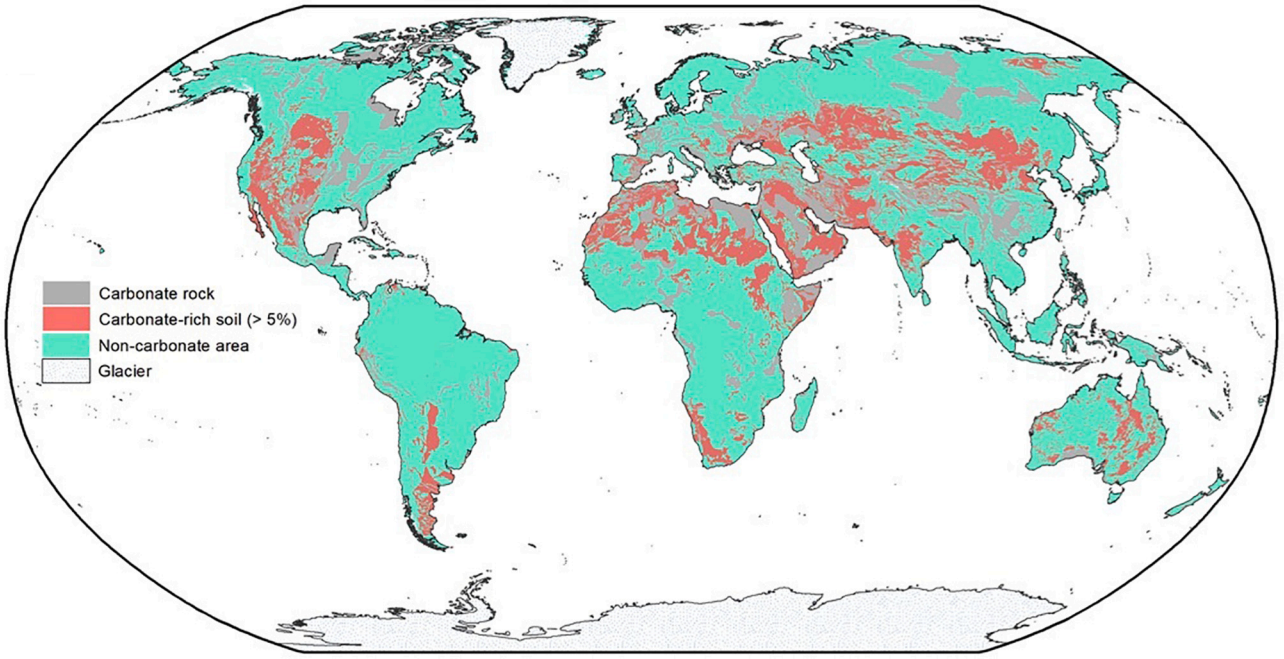

Fig. 3. Global distribution of carbonate rocks, and carbonate-rich soils (carbonate>5%) in non-carbonate rock areas.

three ways: (1) changing the temperature-dependent chemical reaction constants (Dreybrodt, 1988); (2) controlling the vegetation productivity and soil respiration (Gwiazda and Broecker, 1994); (3) altering the water yield via plant evapotranspiration (Zeng et al., 2017). In summary, a warming climate will enhance the soil pCO_2 while lowering carbonate solubility. Hence, there exists a counterbalancing effect between thermodynamics and soil pCO_2 during warming. Over the past few decades, significant soil respiration increases have been detected in the higher latitudes (Huang et al., 2020). In the three simulations, the concentration ($[HCO_3^-]$) in high latitudes or high altitudes significantly increases because of warming (Supplementary Data Fig. 1). The exponential increases of soil pCO_2 modeled in cool temperature zones can explain this $[HCO_3^-]$ increase. By contrast, temperatures in the tropics become extremely high and plant productivity is predicted to be constrained in this over-heated environment in the future (Zeng et al., 2021). The warming temperature will decrease carbonate weathering in subtropical and tropical areas as the soil pCO_2 effect is weak (Zeng et al., 2021). The negative effects of increasing temperature are constant for bare (unvegetated) surfaces in all latitudes (desert, bare rock, bare soil, urban) because few biotic processes can respond significantly to warming there. Thus, our results found a broadly negative correlation between *CCRF* and temperature in the tropical and subtropical regions, while there was a significant positive correlation in the boreal ecosystems (Fig. 6B). In addition, increasing temperatures promote evapotranspiration, thereby reducing water yields. The *CCRF* in arid regions will further be constrained by a warming climate. Regardless of temperature, ready access to water is the most important driver of *CCRF* (Zeng et al., 2019; Zeng et al., 2021). Due to the rapid kinetics of carbonate dissolution, the carbonate system can reach the equilibrium state very quickly (Dreybrodt, 1988). The magnitude of river discharge overwhelms any effects of varying solute concentrations in the inputs (Godsey et al., 2009; Zeng et al., 2016). In addition, being controlled by the balance between temperatures and rates of soil respiration, as shown above, $[HCO_3^-]$ will be more stable than the volume of water flow

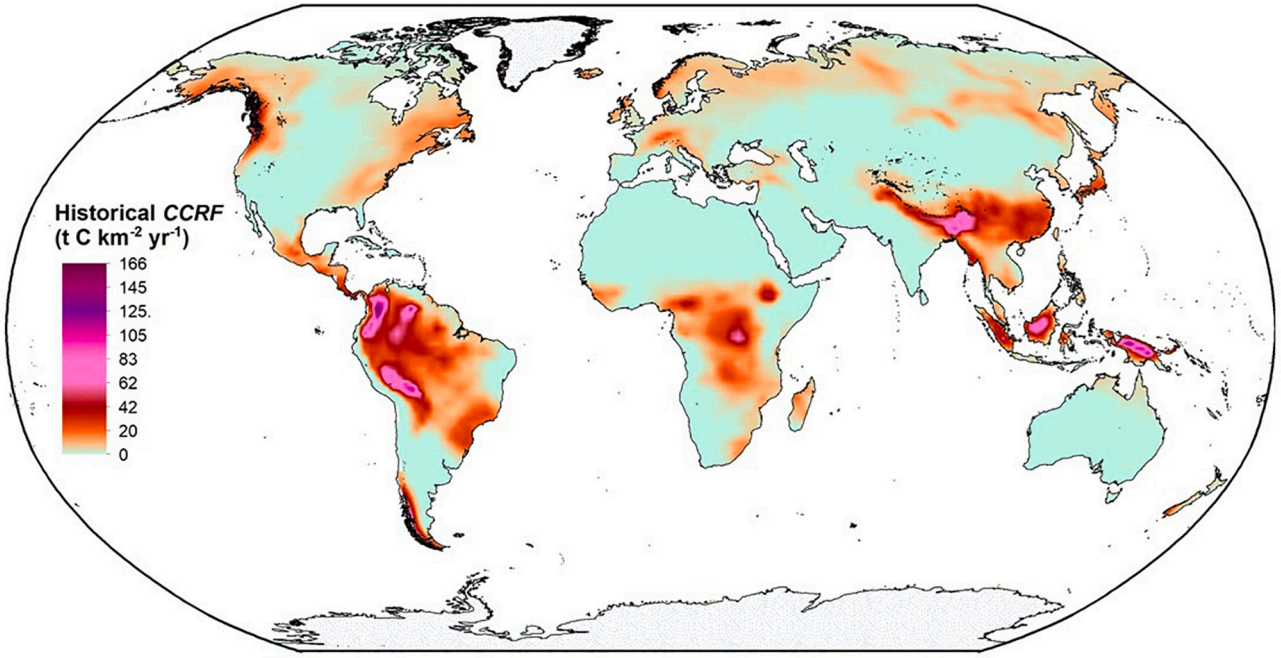

Fig. 4. Historical carbonate weathering carbon removal flux (*CCRF*) over all continent ice-free surfaces, including the carbonate rock areas and non-carbonate rock areas with carbonate-rich soils (carbonate>5%).

Table 2
The top 20 nations for CO_2 removal (*ATCR* or *PCR*) by carbonate weathering.

Nation	*CCRF* (t C km^{-2} yr^{-1})	Carbonate area fraction	*ATCR* (10^6 t C yr^{-1})	*ATCR*/ World total (%)	Nation	*CCRF* (t C km^{-2} yr^{-1})	Non-carbonate area fraction	*PCR* (10^6 t C yr^{-1})	*PCR*/ World total (%)
China	9.15	0.55	47.34	28	Brazil	17.04	0.96	138.29	16
Russia	3.12	0.23	11.88	7	Russia	4.93	0.77	64.40	8
United States	2.22	0.44	9.25	6	Colombia	53.37	0.93	56.18	7
India	6.43	0.36	7.32	4	Canada	6.47	0.79	49.48	6
Peru	23.63	0.22	6.70	4	Democratic Republic of the Congo	22.13	0.90	46.50	6
Papua New Guinea	42.01	0.34	6.60	4	Indonesia	29.30	0.83	45.87	5
Canada	3.15	0.21	6.55	4	China	10.68	0.45	45.24	5
Democratic Republic of the Congo	22.05	0.10	4.98	3	Peru	34.50	0.78	34.75	4
Indonesia	15.47	0.17	4.97	3	United States	6.64	0.56	34.73	4
Mexico	3.82	0.61	4.53	3	Bolivia	34.31	0.92	34.39	4
Colombia	52.46	0.07	4.36	3	India	11.88	0.62	23.13	3
Zambia	19.17	0.24	3.44	2	Venezuela	24.59	0.87	19.55	2
United Republic of Tanzania	9.50	0.32	2.86	2	Burma	28.19	0.81	15.18	2
Brazil	8.02	0.04	2.86	2	Papua New Guinea	40.78	0.66	12.50	1
Bolivia	33.65	0.08	2.83	2	Ecuador	51.27	0.92	12.07	1
Burma	16.99	0.19	2.20	1	Chile	16.27	0.88	10.32	1
Nigeria	6.33	0.38	2.17	1	Central African Republic	16.68	1.00	10.31	1
Sudan	1.89	0.45	2.12	1	Mexico	10.87	0.39	8.40	1
France	6.63	0.56	2.04	1	Ethiopia	12.04	0.58	7.94	1
Paraguay	15.18	0.31	1.87	1	Cameroon	17.97	0.95	7.91	1

CCRF: carbonate-weathering carbon removal flux. *ATCR*: actual total carbon removal in both carbonate rock area and carbonate-rich soils (>5%) in non-carbonate rock area. *PCR*: potential carbon removal in non-carbonate area by liming or spreading of carbonate powders.

(surface and underground) under the climatic perturbations. Globally, the amount of precipitation was positively related with *CCSF* everywhere except in the arid regions with no runoff (Fig. 6A), indicating the crucial role of water supply for carbonate weathering flux control.

Anthropogenic factors are another key driver of carbonate weathering, especially in the regions where human activity has radically changed the land-use. Land-cover change impacts soil respiration (*Rs*) by altering the plant species composition, vegetation structure, soil properties and microclimate (Alekseev et al., 2018; Thomas et al., 2018). Natural vegetation generates higher [HCO_3^-] than cropland or bare plowed land but also lowers the water yield to streams because of its greater evapotranspiration (Zeng et al., 2017). The total carbonate weathering loads depend on the balance between these competing processes. Previous studies found that agricultural water management

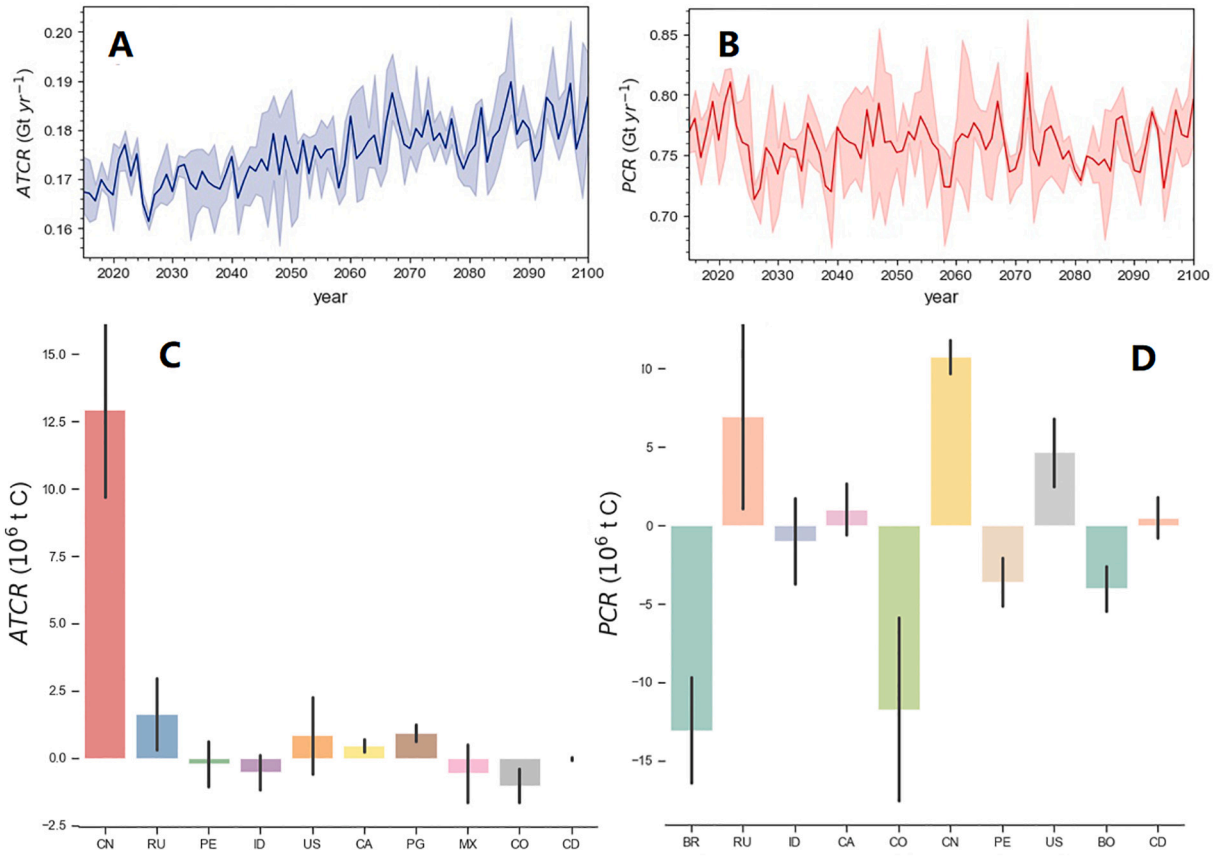

Fig. 5. Global trends of actual total carbon removal (*ATCR*) and potential carbon removal (*PCR*) by carbonate weathering in the 21st Century. (A) the average *ATCR* trend from 2015 to 2100; shaded area shows the 95% confidence interval of three CMIP6 scenarios (ssp126, ssp245, ssp585). (B) the average *PCR* trend from 2015 to 2100. (C) the net changes of *ATCR* in the top 10 countries with highest *ATCR* in future estimations. (D) the net changes of *PCR* in the top 10 countries with highest *PCR* in our future estimates.

increased the aqueous HCO_3^- export by enhancing river discharge (Raymond et al., 2008). Indeed, cropland may generate higher carbonate weathering loads than natural vegetation or bare land, because its soil water flow and HCO_3^- can both reach a high level (Zeng et al., 2017). However, the impact of land cover changes can vary between different temperature zones. Land-cover is more important for the total soil respiration in boreal and temperate regions, due to the considerable productivity and respiration rate differences between forest and non-forest ecosystems in this temperature-sensitive zone (Huang et al., 2020). In contrast, the pCO_2 effect on [HCO_3^-] will be weaker in tropical high temperature environments. The ACCESS CMIP6 GCM parameters considered the role of land cover. Our simulations showed that the spatial variations of *CCRF* are significantly correlated with fraction of cropland cover in some global regions (Fig. 6C). An earlier study also suggested that the modern agricultural expansion in the tropics accounts for 50% of total carbon removal change (Zeng et al., 2019). To simply quantify the influences of human land-uses policies on *CCRF* in different areas, we plotted the future *CCRF* trends under a drastic warming scenario (+5 °C), and estimated their responses to different land-use change scenarios (Fig. 7). These future projections were estimated separately for temperate and subtropical/tropical conditions. We fixed infiltration rates for different land uses and set an initial annual precipitation of 600 mm. The soil pCO_2 of forests was calculated by the methods of our previous simulation (Zeng et al., 2019). Under a drastic warming scenario, reforestation of temperate bare land (urban→forest, +10% per °C) will likely enhance the *CCRF*, while land-use conversion from cropland to forest may lower the flux of HCO_3^- (Fig. 7). These two experiments indicated that agricultural activities may lead to a higher *CCRF* in spite of [HCO_3^-] decline during forest loss, while urbanization will drastically reduce the weathering loads. The rising water yield cannot compensate for the relatively drastic [HCO_3^-] decline of *CCRF* in bare lands. The mean [HCO_3^-] of global non-forest areas was 17% lower than the forest, and the forest [HCO_3^-] was almost twice that of bare land. If there is no land-use change, these relatively drastic warming temperatures are predicted to draw down the *CCRF*, although precipitation is always a positive factor (Fig. 6A). These predictions are consistent with the findings in a carbonate weathering simulation test which suggests croplands produce higher *CCRF* than natural vegetation or bare land due to their greater water yield (Zeng et al., 2017). The consequences of different land uses in the different temperature zones are quite diverse. Thus, we stress that the local conditions should be considered when devising strategies to enhance carbonate weathering.

4.2. Potential large-scale carbon removal by land-use changes

Climate warming will be the fundamental background condition for continental weathering in the coming years. As temperature rises on continental surfaces, carbonate weathering intensity will be constrained by the lowering of CO_2 solubility, especially in the regions without vegetation cover (i.e. the high pCO_2 of deep rooting zones elsewhere will be close to the open atmospheric level here, Zeng et al., 2021). Thus, the primary target to achieve increase of the *CCRF* in both carbonate and non-carbonate terrains is to restore the local ecology by means of forestation or cultivation. According to our estimates, if the global bare lands (exclude currently glaciated continental regions) are replaced by grassland or cropland, the total carbon removal (*ATCR* + *PCR*) could be enhanced by approximately 0.12 Gt yr^{-1}, which is equivalent to ~73% of the recent global *ATCR*. Our simulation indicates that cropland

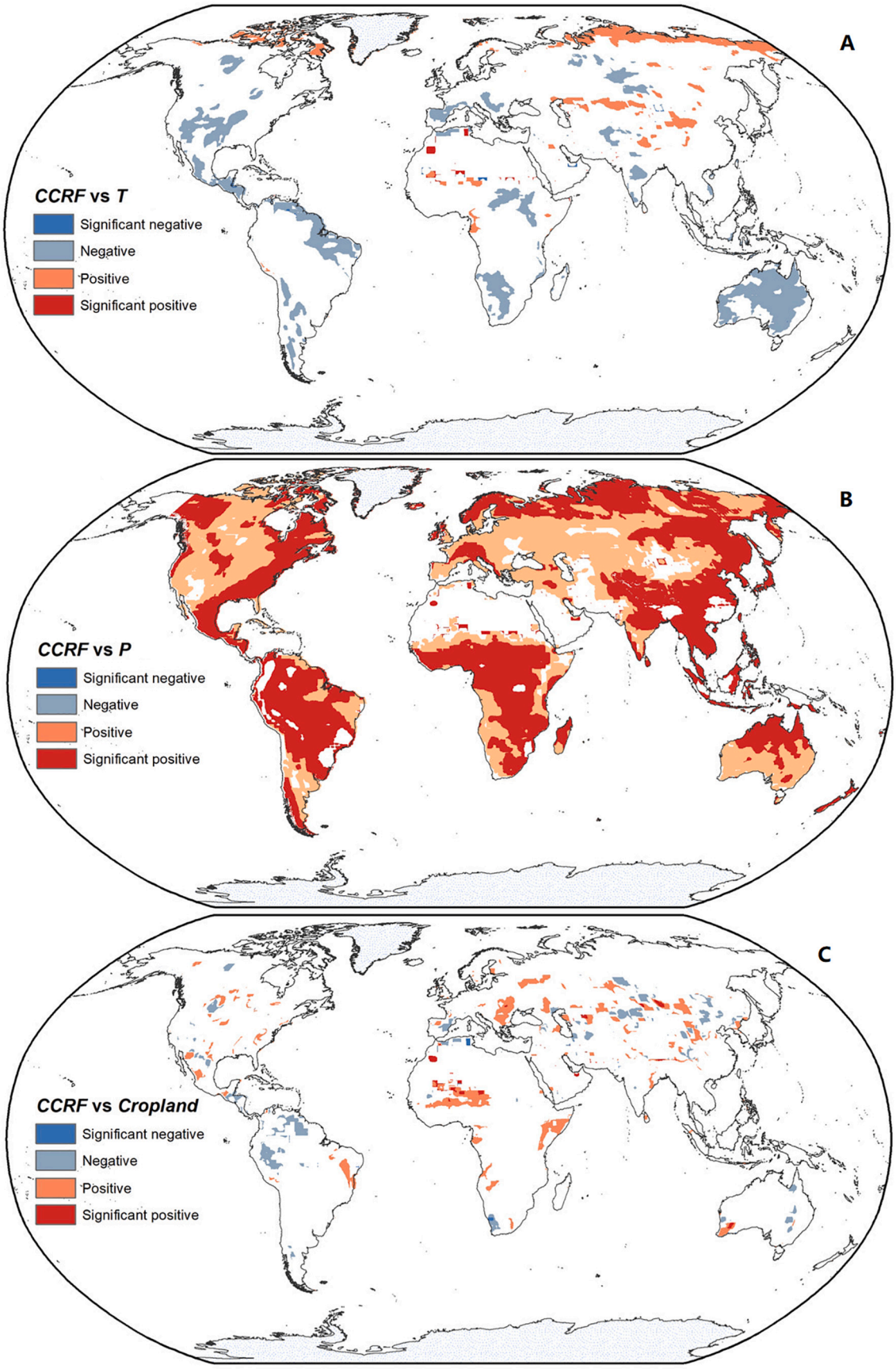

Fig. 6. Spatial patterns of the correlation coefficients between *CCRF* and its driving factors from 2015 to 2100 under the ssp245/RCP4.5 future scenario. (A) *CCRF* and precipitation (*P*), (B) *CCRF* and temperature (*T*), (C) *CCRF* and cropland fraction (areas of significant precipitation decrease were excluded). All the labeled areas pass the 0.05 significance level. Significant negative/positive were the areas with $R^2 > 0.7$, and negative/positive were the areas with $0.25 < R^2 < 0.7$.

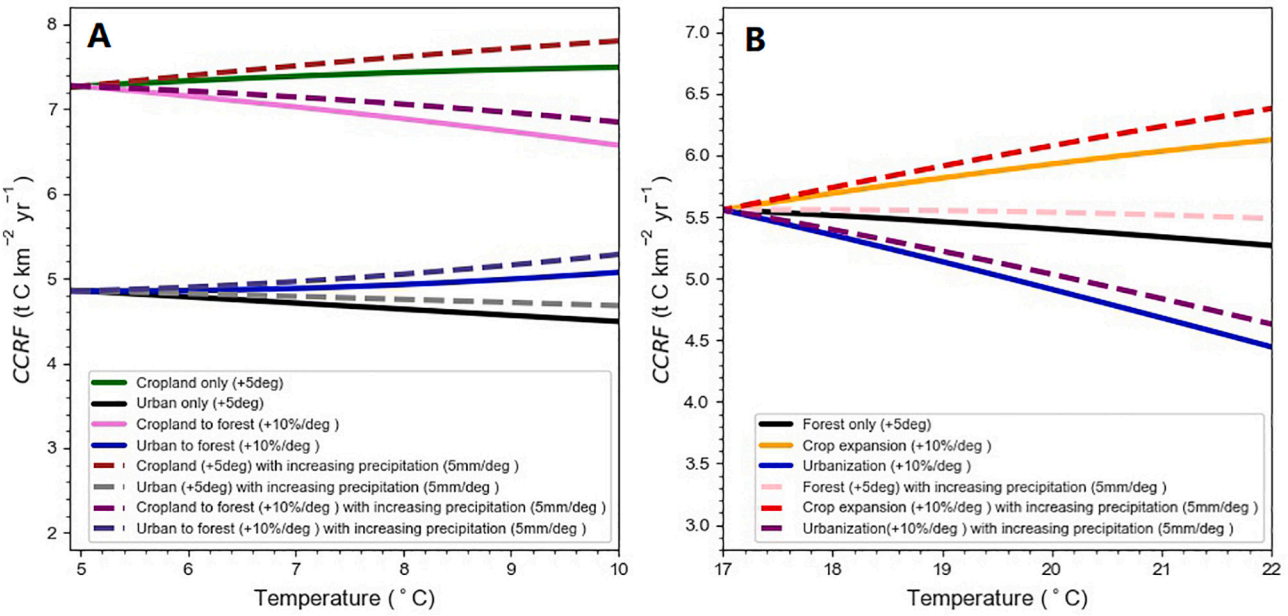

Fig. 7. Variations in the carbonate weathering carbon removal flux (*CCRF*) under different projected future climate and land-use change scenarios. The *CCRF* in temperate and in tropical/sub-tropical settings were simulated separately for five future temperature increases, with or without increasing precipitation. (A) shows the *CCRF* variations in a temperate climate with two reforestation scenarios, cropland→forest and urban→ forest, simulated under different precipitation conditions. We assumed that each degree of temperature increase will be accompanied by 10% of land-use conversion from cropland/urban to forest (forest fraction: left→right, 0% → 50%). The scenarios with no land-cover change are also presented. (B) shows the *CCRF* variations in a sub-tropical or tropical climate with two deforestation scenarios, cropland expansion and urbanization, simulated under different precipitation conditions. We assumed that each degree of temperature increase will be accompanied by 10% of forest loss (left→right, 100% → 50%) to cropland or urban (initial: 0%). Here, the infiltration rates of forest, cropland, urban settings were fixed at 0.35, 0.55 and 0.8 respectively. Initial precipitation was set at 600 mm yr^{-1}. The cropland pCO_2 is set to half of the forest value. The pCO_2 of the atmosphere was fixed at 400 ppmv.

generates higher *CCRF* than forest due to its higher water yield, yet deforestation may not be an advisable practice to enhance the carbonate weathering flux because forest loss decreases the carbon removal captured by plants. Thus, it is not suggested that *CCRF* be promoted via reclamation, especially in temperate or boreal forest regions. Instead, better utilization of the water resources in existing croplands may be the best strategy. Yet, the increasing population in tropical regions has already substantially destroyed nature rainforest and expanded cropland areas (DeFries et al., 2010). We suggest that there is a great opportunity for increasing *PCR* via agriculture liming where the land-use change trends seem irreversible in these areas. In past decades, agricultural activity has increased the carbonate weathering intensity and alkalinity flux in global rivers (Raymond et al., 2008; Drake et al., 2018). Irrigation increases the discharge through cropland by diverting water flow from other kinds of land cover and/or by extracting groundwater. This extra water supply can lead to more abundant water-mineral interactions in croplands, thereby potentially enhancing downstream HCO_3^- loads (Raymond et al., 2008). For some arid or semi-arid regions where there are rich pedogenic calcites, irrigation will increase the amount of water circulating through cultivated watersheds. River water reuse in these watersheds will strongly promote the carbonate weathering flux in arable soils. Further, water circulating in non-carbonate terrain is typically very undersaturated to calcite and thus can be a great resource for enhancing bicarbonate production by changing cropland practices. Liming combined with centralized water irrigation could considerably lower the costs and energy needs. Thus, such water management on croplands has great carbon removal potential.

4.3. Carbon removal uncertainties caused by non-carbonic acids and closed system condition

To reach potential CO_2 removal goal via global non-carbonate area liming is rewarding, but it is also necessary to discuss the negative influences of other natural and anthropogenic factors on this treatment. Compared with carbonic acid (week acid), nitric and sulfuric acids (strong acids) also lead minerals dissolution and contribute alkalinity to the ocean. Unlike natural carbonate weathering process by carbonic acid, strong acid dissolution inversely generates CO_2 and lowers the carbon removal capacity (Martin, 2017). Therefore, it may result in uncertainty when we estimate the potential CO_2 removal by future non-carbonate area liming strategy, especially considering the anthropogenic S and N emissions have been increasing globally since industrial revolution. Nitric acids in the soil could be formed by human agriculture ammonia-based fertilizer applications and atmospheric NH_x depositions. The oxidation of reduced forms of nitrogen (NH_4^+/NH_3) generates acids (NH_4^+ can be exchanged for a proton on a soil surface, taken up by plants or be nitrified by microbes) (Galloway, 1995), which should dissolve carbonates minerals (Martin, 2017). Many intermediate phases occur during oxidation of NH_4^+, which can be described by (Robertson and Groffman, 2007):

$$NH_4^+ + 2O_2 \rightarrow HNO_3 + H_2O + H^+ \quad (8)$$

The nitric acid dissolve the carbonate minerals can be expressed as:

$$2HNO_3 + CaCO_3 \rightarrow Ca^{2+} + 2NO_3^- + CO_2 + H_2O \quad (9)$$

Sulfuric acid is another strong acid that produces CO_2. This acid is generated by different sources such as pyrite oxidative weathering and the oxidation of atmospheric SO_2 deposition, which can be represented by (Li et al., 2008):

$$FeS_2 + 15/4O_2 + 7/2H_2O \rightarrow Fe(OH)_3 + 2SO_4^{2-} + 4H^+ \quad (10)$$

$$SO_2 + 2OH \rightarrow H_2SO_4 \rightarrow SO_4^{2-} + 2H^+ \quad (11)$$

$$SO_2 + H_2O_2 \rightarrow H_2SO_4 \rightarrow SO_4^{2-} + 2H^+ \quad (12)$$

Weathering of carbonate minerals by sulfuric acid can be represented by:

$$H_2SO_4 + 2CaCO_3 + H_2O \rightarrow CaCO_3 + CaSO_4 \cdot 2H_2O + CO_2 \quad (13)$$

Previous studies calculated the contribution of oxidative nitrogenous fertilizer induced carbonate dissolution to croplands in global carbonate outcrops (~3.45 × 10^6 km^2), indicating this anthropogenic factor may decrease the CO_2 removal by about 1.3–3.4 Tg C yr^{-1} (Perrin et al., 2008). Based on the new global carbonate area classification in this study (carbonate rocks + carbonate rich soil), we extended this area to around 5.80 × 10^6 km^2 and estimate that CO_2 removal will decrease by about 2.36–5.72 Tg C yr^{-1}, accounting for 1.42%–3.45% of historical *ATCS*. Furthermore, approximately 2% of global ice-free land will turn to cropland till 2100 under future RCP4.5 scenario (ACCESS database). If the application of nitrogenous fertilizers for these croplands remains a similar level with the present state and all the non-carbonate regions are fertilized by carbonate rock powders, the CO_2 emission that driven by nitric acids on global arable soils may neutralize 1.40%–3.41% of the global total carbonate weathering CO_2 removal goal (all non-carbonate areas are limed in 2100). This future estimation indicates that increasing croplands may return more CO_2 to atmosphere due to the nitric acid impact, yet this disadvantage is minor and cannot undermine the potential CO_2 removal goal of wide liming strategy. Meanwhile, the lime use on non-carbonate areas also need to account of the ecological benefits such as food production increase, soil carbon stock rise and the soil acidification recovery, which may further offset its negative impacts.

Previous studies estimated that the sulfuric acid production by oxidative weathering of pyrite may contribute nearly 5% of Phanerozoci carbonate mineral dissolution (Berner et al., 1983). This may also result in uncertainty for estimating ATCR and PCR. However, such oxidative weathering processes are mainly occur from point sources, which could be highly random globally. Thus, we will not discuss its impacts for global liming strategy.

Acid deposition occurred as one of the most public environmental issues during the 1970s–1980s (Driscoll et al., 2001). The strong acids from acid deposition should dissolve carbonate rocks, decreasing the CO_2 removal capacity. Globally, human emitted 50Tg N/yr NH_x and 100Tg S/yr SO_2 to atmosphere (Galloway, 1995). These emissions are equally divided and deposited between continents and oceans. Therefore, if we assume an extreme situation that all the deposited NH_x and SO_2 are oxidated, and half of the deposited acids react with carbonate minerals on continental surface (another half dissolve silicate minerals). In this case, the CO_2 removal through global ice-free land (after spreading lime) will decrease by around 2.97% (1.86% for SO_2 and 1.11% for NH_x). Lerman et al. (2007) estimated that anthropogenic emissions of SO_2 to the atmosphere, as projected for the future and at the upper bound of the projection, may provide sulfuric acid to the continental surface that is 3 to 5 times greater than the natural production by the oxidation of pyrite in sediments. These authors further concluded that the higher input rates of sulfuric acid may increase the dissolved ionic solid concentrations in river waters by about 13% but without significantly affecting the CO_2 consumption in weathering. Moreover, due to the air pollution control in US and Europe, the emission of SO_2 and NO_x have significantly reduced after 1990s (Templer et al., 2012; Lawrence et al., 2012). Meanwhile, NH_x emissions are unlikely to decrease and is projected double in the next century because of growing demand of agriculture (Templer et al., 2012; Galloway et al., 2004; Galloway et al., 2008). However, the NH_x emission may not only have negative effect for terrestrial CO_2 capture. NH_x deposition alleviates nitrogen limitation of productivity in terrestrial ecosystem and increase global terrestrial carbon storage of between 1.5 and 2.0 Gt yr^{-1} (Holland et al., 1997), which is much higher than the nitric acid induced CO_2 emissions.

The closed system condition may draw down the equilibrium concentration due to the decreasing pCO_2 in deep flow (Dreybrodt, 1988). The reduced $[HCO_3^-]_{eq}$ may influence the magnitude of CO_2 removal and result in uncertainty. However, it's still had no plausible principles to clear define the boundary of open and close system conditions. Here, to experimentally estimate the potential CO_2 removal uncertainty that caused by this factor, we apply a global soil depth database ISRIC-WISE v3.0 and use a similar hypothesis that initially given by Romero-Mujalli et al. (2019). The soil depth under 140 cm is set to close-system condition control. Therefore, the crossed spatial analysis indicates that 13.8% of carbonate outcrops with low soil carbonate content (<5%) may be affected by closed systems, which may potentially lower the *ATCR* by about 5.22% (~0.86% for *ATCR* + *PCR*). Meanwhile, we believe it's too early (no solid evidence) to conclude that closed system conditions would impact limed soils. The spreading of carbonate rock powders via aircraft or drone may not likely impact the deep soil layers (>140 cm). The drainage water through limed soils may reach equilibrium with the soil pCO_2 at root zone, which can be seen as open system. Hence, due to the potential minor influences of closed-system conditions, we suggest it is too early to account for this factor for the future liming strategy.

4.4. Potential cost and concerns of liming strategy

Limestone and dolomite are two common carbonate rocks which have been mined, ground, and applied in different areas as liming materials to counteract ecosystem acidification (Smallidge et al., 1993; Huettl and Zoettl, 1993; Moore et al., 2012). This is due to their low cost, easy handling, and low contaminant content (Henrikcson et al., 1995). To apply to global non-carbonate area liming treatment requires large amount of these carbonate rocks. Our modeling predicts that widespread use of lime (limestone or dolomite powders) for all non-carbonate landscapes can generate five times the current *ATCR*. However, this treatment would require great labor resources for lime ($CaCO_3$ powder) production and energy costs for spreading. To reach this potential CO_2 removal, approximately 7.0 Gt of $CaCO_3$ powders need be generated and spread each year. Thus, the first concern of this strategy is the current global lime production capacity. If it cannot meet the requirement, more limestone quarries, lime factories and lime transportation are expected. If we set the global average cost of industrial lime fertilizer is 24.26$ per ton, the US reference lime price given by Bongiovanni and Lowenberg-Deboer (2000) (including transportation). The minimum cost for globe lime production thus reaching 170 billion $ per year. Extra CO_2 emission may also occur during the mining, crushing, grinding of carbonate rocks, and this negative impact should be well estimated in the future. Another concern is the cost of lime spreading. Conventionally, lime has been distributed by economical methods such as mechanical spreader pulled by tractors or vehicles (Côté and Ouimet, 1996). To reach remote place such as forest, lake and stream, lime has normally been applied by airplane, helicopter or drone (Huettl and Zoettl, 1993; Hudy et al., 2000; Battles et al., 2014). The prices and energy cost of different areas and spreading methods may vary widely. Hence, it is difficult to calculate a total amount of this cost. To lower the cost of spreading lime, here we suggest an alternative, more efficient approach that is to focus on the regions which had high *CCRF* in the historical period (Fig. 4). This alternative could further lower the spreading costs. Our historical simulation results have demonstrated that the lands between latitudes 15°S - 15°N contain nearly 53% of global *PCR*, yet they are only 29% of global non-carbonate terrain (Fig. 8). Therefore, spreading lime on these tropical regions may be the first priority.

Although, liming mitigates soil acidification (Goulding, 2016), increases crop production (Caires et al., 2006) and organic carbon storage (Paradelo et al., 2015) and brings other environmental improvements (Moore et al., 2012) which could enhance CO_2 removal while benefit the ecology. Yet, liming treatments are not always ecological-friendly for ecosystems. Some plants species may benefit from lime treatment, but some may not be affected or even have negative effects on their survival and growth (Long et al., 2011). Moreover, there are other ecological

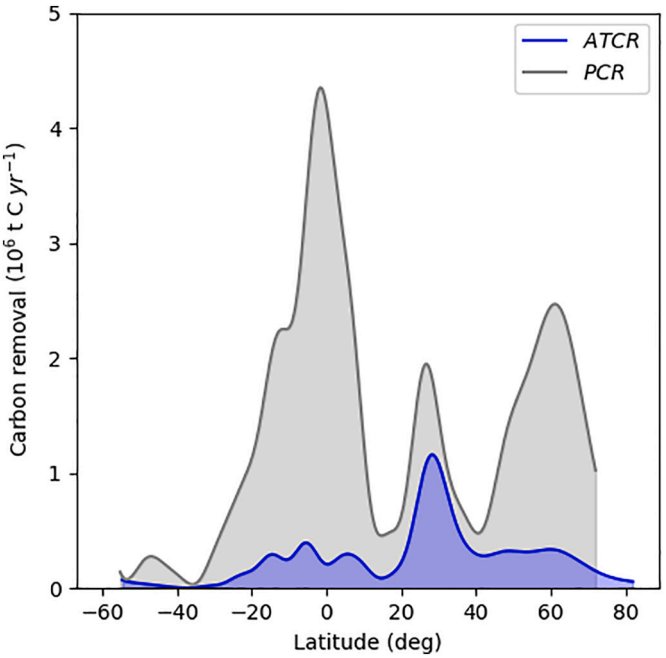

Fig. 8. The latitudinal distributions of carbon removal by carbonate weathering. *ATCR:* actual total carbon removal; *PCR:* potential carbon removal in the historical period of record, 2000–2014.

side-effects of liming, including changes in soil properties, soil microbes and soil fauna. For instance, studies detect that long-term liming treatment for forest soils may stimulate fine root development, increase the danger of frost and drought damage, arise earthworm invasion risk (Huettl and Zoettl, 1993; Homan et al., 2016). Indeed, the choice of liming as a carbon capture tool should not only weigh its atmospheric CO_2 removal potential, but also consider the local ecology health and balance. Healthy soils, vegetation, water resources and the atmospheric CO_2 sink by carbonate weathering are highly related (Goldscheider, 2019). Therefore, the different plant adaptations of soil lime content and other accompanying side-effects need to be fully evaluated in regional scale before use this strategy. Finally, different CO_2 emissions will determine future warming trends and the environmental perturbations they induce, so the responses of additional carbonate weathering may also vary widely. However, CO_2 removal by deliberate land-use practices such as land cover regulation, water management, fertilizer use strategy may make it easier to account for these uncertainties. Therefore, we stress that carbonate weathering enhancement by land-use changes can potentially help mitigate the current climate trends and reach the carbon neutral goal in 2050 (Mallapaty, 2020).

5. Conclusions and future work

We have used a new global carbonate area classification and modeling approach to estimate the actual total carbon removal (*ATCR*) and potential total carbon removal (*PCR*) of carbonate weathering at the global scale. The new *ATCR* estimation was calculated from the known global outcrop of carbonate rocks and a best estimate of the extent of carbonate-rich soils in non-carbonate rock areas. It is approximately 0.166 Gt C yr^{-1}, similar to a previous estimate based on a global river solute load database. The soil carbonate threshold for carbonate weathering control of river discharge is set at 5%. *PCR* is the carbon removal potential, which could be attained by spreading crushed carbonate minerals (lime) on non-carbonate soils. We found that this land-use change may result in 0.843 Gt more carbon removal per year. Our simulation implies that the global variations of carbonate weathering carbon removal flux involve the interaction of climatic change and human land-use dynamics. Future carbonate weathering land-use enhancement strategies should consider the climatic and vegetation conditions of the different regions. Liming on non-carbonate landscapes to increase *PCR* needs to focus on the areas with higher carbon removal efficiency, in order to lower the economic and energy costs. We stress that this liming practice may well be an effective tool, offering five times more carbon removal than by existing carbonate weathering, which highlights the potential role of this strategy to help society reach carbon neutral conditions by mid-century.

Declaration of Competing Interest

The authors declare that they have no known competing financial interests or personal relationships that could have appeared to influence the work reported in this paper.

Acknowledgments

Special thanks are given tssso Prof. Dr. Derek Ford (McMaster University, Canada) for his thoughtful comments and corrections, which greatly improved the original draft. This study was financially supported by the Strategic Priority Research Program of Chinese Academy of Sciences (XDB40020000), the National Natural Science Foundation of China (42130501, 42141008, U1612441 and 41921004).

Appendix A. Supplementary data

Supplementary data to this article can be found online at https://doi.org/10.1016/j.earscirev.2021.103915.

References

Adams, J.M., 1993. Caliche and the carbon cycle. Nature 361, 213–214.
Alekseev, A., Alekseeva, T., Kalinin, P., Hajnos, M., 2018. Soils response to the land use and soil climatic gradients at ecosystem scale: mineralogical and geochemical data. Soil Tillage Res. 180, 38–47.
Battles, J.J., Fahey, T.J., Driscoll Jr., C.T., Blum, J.D., Johnson, C.E., 2014. Restoring soil calcium reverses forest decline. Environ. Sci. Technol. Lett. 1, 15–19.
Beaulieu, E., Goddéris, Y., Donnadieu, Y., Labat, D., Roelandt, C., 2012. High sensitivity of the continental-weathering carbon dioxide sink to future climate change. Nat. Clim. Chang. 5, 46–349.
Berner, E.K., Berner, R.A., 2012. Global Environment: Water, Air, and Geochemical Cycles. Princeton University Press.
Berner, R.A., Garrels, A.C., Garrels, R.M., 1983. The carbonate-silicate geochemical cycle and its effect on atmospheric carbon-dioxide over the past 100 million years. Am. J. Sci. 283, 641–683.
Blum, J.D., Gazis, C.A., Jacobson, A.D., Chamberlain, C.P., 1998. Carbonate versus silicate weathering in the Raikhot watershed within the high Himalayan crystalline series. Geology 26, 411–414.
Bongiovanni, R., Lowenberg-Deboer, J., 2000. Economics of variable rate lime in Indiana. Precis. Agric. 2, 55–70.
Caires, E.F., Barth, B., Garbuio, F.J., 2006. Lime application in the establishment of a no-till system for grain crop production in Southern Brazil. Soil Tillage Res. 89, 3–12.
Côté, B., Ouimet, R., 1996. Decline of the maple-dominated forest in southern Quebec: impact of natural stresses and forest management. Environ. Rev. 4, 133–148.
Das, A., Krishnaswami, S., Sarin, M.M., Pande, K., 2005. Chemical weathering in the Krishna Basin and Western Ghats of the Deccan Traps, India: rates of basalt weathering and their controls. Geochim. Cosmochim. Acta 69, 2067–2084.
DeFries, R.S., Rudel, T., Uriarte, M., Hansen, M., 2010. Deforestation driven by urban population growth and agricultural trade in the twenty-first century. Nat. Geosci. 3, 178–181.
Drake, T.W., Tank, S.E., Zhulidov, A.V., Holmes, R.M., Gurtovaya, T., Spencer, R.G.M., 2018. Increasing alkalinity export from large Russian Arctic rivers. Environ. Sci. Technol. 52, 8302–8308.
Dreybrodt, W., 1988. Processes in Karst Systems. Springer, Berlin.
Driscoll, C.T., Lawrence, G.B., Bulger, A.J., Butler, T.J., Cronan, C.S., Eagar, C., 2001. Acidic deposition in the northeastern United States: sources and inputs, ecosystem effects, and management strategies. BioScience 51, 180–198.
Einsele, G., Yan, J., Hinderer, M., 2001. Atmospheric carbon burial in modern lake basins and its significance for the global carbon budget. Glob. Planet. Chang. 30, 167–195.
Florides, G.A., Christodoulides, P., 2009. Global warming and carbon dioxide through sciences. Environ. Int. 35, 390–401.
Fornara, D.A., Steinbeiss, S., McNamara, N.P., Gleixner, G., Oakley, S., Poulton, P.R., Macdonald, A.J., Bardgett, R.D., 2011. Increases in soil organic carbon sequestration can reduce the global warming potential of long-term liming to permanent grassland. Glob. Chang. Biol. 17, 1925–1934.

Gaillardet, J., Dupré, B., Louvat, P., Allegre, C., 1999. Global silicate weathering and CO_2 consumption rates deduced from the chemistry of large rivers. Chem. Geol. 159, 3–30.
Gaillardet, J., Calmels, D., Romero-Mujalli, G., Sakarova, E., Hartmann, J., 2019. Global climate control on carbonate weathering intensity. Chem. Geol. 527. UNSP 118762.
Galloway, J.N., 1995. Acid deposition: Perspectives in time and space. Water Air Soil Pollut. 85, 15–24.
Galloway, J.N., Dentener, F.J., Capone, D.G., Boyer, E.W., Howarth, R.W., Seitzinger, S. P., 2004. Nitrogen cycles: past, present, and future. Biogeochemistry 70, 153–226.
Galloway, J.N., Townsend, A.R., Erisman, J.W., Bekunda, M., Cai, Z., Freney, J.R., et al., 2008. Transformation of the nitrogen cycle: recent trends, questions, and potential solutions. Science 320, 889–892.
Gislason, S.R., Oelkers, E.H., Eiriksdottir, E.S., Kardjilov, M.I., Gisladottir, G., Sigfusson, B., Snorrason, A., Elefsen, S., Hardardottir, J., Torssander, P., Oskarsson, N., 2009. Direct evidence of the feedback between climate and weathering. Earth Planet. Sci. Lett. 277, 213–222.
Goddéris, Y., Williams, J.Z., Schott, J., Pollard, D., Brantley, S.L., 2010. Time evolution of the mineralogical composition of Mississippi Valley loess over the last 10kyr: climate and geochemical modelling. Geochim. Cosmochim. Acta 74, 6357–6374.
Godsey, S.E., Kirchner, J.W., Clow, D.W., 2009. Concentration-discharge relationships reflect chemostatic characteristics of US catchments. Hydrol. Process. 23, 1844–1864.
Goldscheider, N., 2019. A holistic approach to groundwater protection and ecosystem services in karst terrains. Carbonates Evaporites 34, 1241–1249.
Goldscheider, N., Chen, Z., Broda, S., Auler, A.S., Bakalowicz, M., Drew, D., Hartmann, J., Jiang, G., Moosdorf, N., Stevanovic, Z., Veni, G., 2020. Global distribution of carbonate rocks and karst water resources. Hydrogeol. J. 28, 1661–1677.
Goulding, K.W.T., 2016. Soil acidification and the importance of liming agricultural soils with particular reference to the United Kingdom. Soil Use Manag. 32, 390–399.
Gwiazda, R.H., Broecker, W.S., 1994. The separate and combined effects of temperature, soil pCO_2 and organic acidity on silicate weathering in the soil environment: formulation of a model and results. Glob. Biogeochem. Cycles 8, 141–155.
Hagedorn, B., Cartwright, I., 2010. The CO_2 system in rivers of the Australian Victorian Alps: CO_2 evasion in relation to system metabolism and rock weathering on multi-annual time scales. Appl. Geochem. 25, 881–899.
Hain, M.P., Sigman, D.M., Haug, G.H., 2014. The Biological Pump in the Past in Treatise on Geochemistry, 2nd ed. Elsevier, pp. 485–517.
Hamilton, S.K., Kurzman, A.L., Arango, C., Jin, L.X., Robertson, G.P., 2007. Evidence for carbon sequestration by agricultural liming. Glob. Biogeochem. Cycles 20, GB1008.
Haynes, R.J., Naidu, R., 1998. Influence of lime, fertilizer and manure applications on soil organic matter content and soil physical conditions: a review. Nutr. Cycl. Agroecosyst. 51, 123–137.
Henrikcson, L., Hindar, A., Thörnelöf, E., 1995. Freshwater liming. Water Air Soil Pollut 85, 131–142.
Holland, E.A., Braswell, B.H., Lamarque, J., Townsend, A., Sulzman, J., Müller, J., Dentener, F., Brasseur, G., Levy, H., Penner, J.E., Roelof, G., 1997. Variation in the predicted spatial distribution of atmospheric nitrogen deposition and their impact on carbon uptake by terrestrial ecosystems. J. Geophys. Res. 102, 15849–15866.
Homan, C., Beier, C., McCay, T., Lawrence, G., 2016. Application of lime ($CaCO_3$) to promote forest recovery from severe acidification increases potential for earthworm invasion. For. Ecol. Manag. 368, 39–44.
Hu, D., Liu, C., Zhao, Z., Li, S., Lang, Y., Li, X., Hu, J., Liu, B., 2017. Geochemistry of the dissolved loads of the Liao River basin in Northeast China under anthropogenic pressure: chemical weathering and controlling factors. J. Asian Earth Sci. 138, 657–671.
Huang, N., Wang, L., Song, X., Black, T.A., Jassal, R.S., Myneni, R.B., Wu, C., Wang, L., Song, W., Ji, D., Yu, S., Niu, Z., 2020. Spatial and temporal variations in global soil respiration and their relationships with climate and land cover. Sci. Adv. 6, eabb8508.
Hudy, M., Downey, D.M., Bowman, D.W., 2000. Successful restoration of an acidified native brook trout stream through mitigation with limestone sand. N. Am. J. Fish Manag. 20, 453–466.
Huettl, R.F., Zoettl, H.W., 1993. Liming as a mitigation tool in Germany declining forests - reviewing results from former and recent trials. Forest Ecol. Manag 61, 325–338.
Huntington, T.G., 2006. Evidence for intensification of the global water cycle: review and synthesis. J. Hydrol. 319, 83–95.
Jacobson, A.D., Blum, J.D., Chamberlain, C.P., Poage, M.A., Sloan, V.F., 2002. Ca/Sr and Sr isotope systematics of a Himalayan glacial chronosequence: carbonate versus silicate weathering rates as a function of landscape surface age. Geochim. Cosmochim. Acta 66, 13–27.
Law, R.M., Ziehn, T., Matear, R.J., Lenton, A., Chamberlain, M.A., Stevens, L.E., Wang, Y., Srbinovsky, J., Bi, D., Yan, H., Vohralik, P.F., 2017. The carbon cycle in the Australian Community climate and earth system simulator (ACCESS-ESM1) - Part 1: model description and pre-industrial simulation. Geosci. Model Dev. 10, 2567–2590.
Lawrence, G.B., Shortle, W.C., David, M.B., Smith, K.T., Warby, R.A.F., Lapenis, A.G., 2012. Early indications of soil recovery from acidic deposition in US red spruce forests. Soil Sci. Soc. Am. J. 76, 1407–1417.
Lerman, A., Mackenzie, F.T., 2005. CO_2 air-sea exchange due to calcium carbonate and organic matter storage, and its implications for the global carbon cycle. Aquat. Geochem. 11, 345–390.
Lerman, A., Wu, L.L., Mackenzie, F.T., 2007. CO_2 and H_2SO_4 consumption in weathering and material transport to the ocean, and their role in the global carbon balance. Mar. Chem. 106, 326–350.
Li, S.L., Calmels, D., Han, G., Gaillardet, J., Liu, C.Q., 2008. Sulfuric acid as an agent of carbonate weathering constrained by $\delta^{13}C$ DIC: examples from Southwest China. Earth Planet. Sci. Lett. 270, 189–199.
Liu, Z., Dreybrodt, W., Wang, H., 2010. A new direction in effective accounting for the atmospheric CO_2 budget: considering the combined action of carbonate dissolution, the global water cycle and photosynthetic uptake of DIC by aquatic organisms. Earth Sci. Rev. 99, 162–172.
Liu, Z., Dreybrodt, W., Liu, H., 2011. Atmospheric CO_2 sink: silicate weathering or carbonate weathering? Appl. Geochem. 26, S292–S294.
Liu, Z., Macpherson, G.L., Groves, C., Martin, J.B., Yuan, D., Zeng, S., 2018. Large and active CO_2 uptake by coupled carbonate weathering. Earth Sci. Rev. 182, 42–49.
Liu, Z., Yan, H., Zeng, S., 2021. Increasing autochthonous production in inland waters as a contributor to the missing carbon sink. Front. Earth Sci. 9, 620513.
Long, R.P., Horsely, S.B., Hall, T.J., 2011. Long term impact of liming on growth and vigor of northern hardwoods. Can. J. For. Res. 41, 1295–1307.
Ma, Z.W., et al., 2014. Carbon sequestration during the Palaeocene-Eocene thermal Maximum by an efficient biological pump. Nat. Geosci. 7, 382–388.
Mallapaty, S., 2020. How China could be carbon neutral by mid-century. Nature 586, 482–483.
Martin, J.B., 2017. Carbonate minerals in the global carbon cycle. Chem. Geol 449, 58–72.
Meybeck, M., 1986. Composition chimique des ruisseaux non pollués de France. Sci. Géolog. Bull. Mém. 39, 3–77.
Moore, J.D., Ouimet, R., Duchesne, L., 2012. Soil and sugar maple response 15 years after dolomitic lime application. For. Ecol. Manag. 281, 130–139.
Nõges, P., Cremona, F., Laas, A., Martma, T., Rõõm, E., Toming, K., Viik, M., Vilbaste, S., Nõges, T., 2016. Role of a productive lake in carbon sequestration within a calcareous catchment. Sci. Total Environ. 550, 225–230.
Oh, N.H., Raymond, P.A., 2006. Contribution of agricultural liming to riverine bicarbonate export and CO_2 sequestration in the Ohio River basin. Glob. Biogeochem. Cycles 20, GB3012.
Oki, T., 1999. The global water cycle. In: Browning, K., Gurney, R. (Eds.), Global Energy and Water Cycles. Cambridge University Press, pp. 10–27.
Paradelo, R., Virto, I., Chenu, C., 2015. Net effect of liming on soil organic carbon stocks: a review. Agric. Ecosyst. Environ. 202, 98–107.
Pattanaik, J.K., Balakrishnan, S., Bhutani, R., Singh, P., 2013. Estimation of weathering rates and CO_2 drawdown based on solute load: significance of granulites and gneisses dominated weathering in the Kaveri River basin, Southern India. Geochim. Cosmochim. Acta 121, 611–636.
Perrin, A.S., Probst, A., Probst, J.L., 2008. Impact of nitrogenous fertilizers on carbonate dissolution in small agricultural catchments: implications for weathering CO_2 uptake at regional and global scales. Geochim. Cosmochim. Acta 72, 3105–3123.
Raymond, P.A., Oh, N.H., Turner, R.E., Broussard, W., 2008. Anthropogenically enhanced fluxes of water and carbon from the Mississippi River. Nature 451, 449–452.
Retallack, G.J., 2005. Pedogenic carbonate proxies for amount and seasonality of precipitation in paleosols. Geology 33, 333–336.
Robertson, G., Groffman, P., 2007. Nitrogen transformations. Soil Microbiol. Ecol. Biochem. 3, 341–364.
Romero-Mujalli, G., Hartmann, J., Borker, J., Gaillardet, J., Calmels, D., 2019. Ecosystem controlled soil-rock pCO_2 and carbonate weathering - Constraints by temperature and soil water content. Chem. Geol. 527, 118634.
Sanchez, P.A., Ahamed, S., Carre, F., Hartemink, A.E., Hempel, J., Huising, J., Lagacherie, P., McBratney, A.B., McKenzie, N.J., Mendonca-Santos, M.D., Minasny, B., Montanarella, L., Okoth, P., Palm, C.A., Sachs, J.D., Shepherd, K.D., Vagen, T.G., Vanlauwe, B., Walsh, M.G., Winowiecki, L.A., Zhang, G.L., 2009. Digital soil map of the world. Science 325, 680–681.
Schlesinger, W.H., 1985. The formation of caliche in soils of the Mojave Desert, California. Geochim. Cosmochim. Acta 49, 57–66.
Sharma, S.K., Subramanian, V., 2008. Hydrochemistry of the Narmada and Tapti Rivers, India. Hydrol. Process. 22, 3444–3455.
Smallidge, P.J., Brach, A.R., Mackun, I.R., 1993. Effects of watershed liming on terrestrial ecosystem processes. Environ. Rev. 1, 157–171.
Sun, X., Mörth, C., Humborg, C., Gustafsson, B., 2017. Temporal and spatial variations of rock weathering and CO_2 consumption in the Baltic Sea catchment. Chem. Geol. 466, 57–69.
Templer, P.H., Pinder, R.W., Goodale, C.L., 2012. Effects of nitrogen deposition on greenhouse-gas fluxes for forests and grasslands of North America. Front. Ecol. Environ. 10, 547–553.
Thomas, D.T., Moore, A.D., Bell, L.W., Webb, N.P., 2018. Ground cover, erosion risk and production implications of targeted management practices in Australian mixed farming systems: Lessons from the grain and Graze program. Agric. Syst. 162, 123–135.

Wang, L., Zhang, L., Cai, W., Wang, B., Yu, Z., 2016. Consumption of atmospheric CO_2 via chemical weathering in the Yellow River basin: the Qinghai-Tibet Plateau is the main contributor to the high dissolved inorganic carbon in the Yellow River. Chem. Geol. 430, 34–44.

West, T.O., McBride, A.C., 2005. The contribution of agricultural lime to carbon dioxide emissions in the United States: dissolution, transport, and net emissions. Agric. Ecosyst. Environ. 108, 145–154.

Zeng, C., Liu, Z., Zhao, M., Yang, R., 2016. Hydrologically-driven variations in the karst process-related carbon sink flux: insights from high-resolution monitoring of three typical karst catchments in the subtropical karst area of SW China. J. Hydrol. 533, 74–90.

Zeng, Q., Liu, Z., Chen, B., Hu, Y., Zeng, S., Zeng, C., Yang, R., He, H., Zhu, H., Cai, X., Chen, J., Ou, Y., 2017. Carbonate weathering-related carbon sink fluxes under different land uses: a case study from the Shawan simulation Test Site, Puding, Southwest China. Chem. Geol. 474, 58–71.

Zeng, S., Liu, Z., Kaufmann, G., 2019. Sensitivity of global carbonate weathering carbon-sink flux to climate and land-use changes. Nat. Commun. 10, 5749.

Zeng, S., Liu, Z., Goldscheider, N., Frank, S., Goeppert, N., Kaufmann, G., Zeng, C., Zeng, Q., Sun, H., 2021. Comparisons on the effects of temperature, runoff, and land-cover on carbonate weathering in different karst catchments: insights into the future global carbon cycle. Hydrogeol. J. 29, 331–345.

Ziehn, T., Lenton, A., Law, R.M., Matear, R.J., Chamberlain, M.A., 2017. The carbon cycle in the Australian Community climate and earth system simulator (ACCESS-ESM1)- Part 2: historical simulations. Geosci. Model Dev. 10, 2591–2614.